Annex V: Monsoons

Coordinating Lead Authors:
Annalisa Cherchi (Italy), Andrew Turner (UK)

Lead Authors:
Paola A. Arias (Colombia), Mathew Barlow (USA), Ruth Cerezo-Mota (Mexico), Joelle Gergis (Australia), Sergey Gulev (Russian Federation), Dabang Jiang (China), Richard G. Jones (UK), Won-Tae Kwon (Republic of Korea), June-Yi Lee (Republic of Korea), Jian Li (China), Wilfried Pokam Mba (Cameroon), Linda Mearns (USA), Lincoln Muniz Alves (Brazil), Aïda Diongue-Niang (Senegal), Sabin Thazhe Purayil (India), Krishnan Raghavan (India), Juan A. Rivera (Argentina), Jessica Tierney (USA), Tianjun Zhou (China)

Contributing Authors:
Josephine Brown (Australia)

Date of Draft:
3 May 2021

Note:
TSU compiled version

AV.1 Introduction

A monsoon refers to a seasonal transition of regimes in atmospheric circulation and precipitation in response to the annual cycle of solar insolation and the distribution of moist static energy (Wang and Ding, 2008; Wang et al., 2014; Biasutti et al., 2018). A global monsoon can be objectively identified based on precipitation contrasts in the solstice seasons to encompass all monsoon regions (Wang and Ding, 2008). In AR5, regional monsoon domains were identified starting from the definition of the global monsoon tailored over the continents and adjacent oceans, as in Kitoh et al. (2013). This Annex contains the definition of the global monsoon as used in AR6 (Section AV.2), it explains the rationale for the different definition of AR6 regional monsoons compared to AR5 (Section AV.3) and provides the definition and basic characteristics of each regional monsoon assessed (Section AV.4).

AV.2 Definition of the global monsoon

The concept of global monsoon (GM) emerged during the second half of the 20th century, representing the leading empirical orthogonal function (EOF) mode of the annual variations of precipitation and circulation in the global tropics and subtropics as a forced response of the coupled climate system to the annual cycle of solar insolation (Wang and Ding, 2008; An et al., 2015; Wang et al., 2017). GM variability represents, to a large extent, changes in the ITCZ and associated Hadley circulation (Wang et al., 2014). Changes in GM have been attributed to both internal variability and external forcings, ranging from interannual to millennial and orbital time scales (Wang et al., 2014, 2017; An et al., 2015; Geen et al., 2020). In AR6, the global monsoon is defined as the area in which the annual range (local summer minus local winter) of precipitation is greater than 2.5 mm/day (Kitoh et al. et al., 2013), and the domain is represented by the black contour in Figure AV.1. Simulation of the global monsoon and its variability is the subject of coordinated modelling experiments in the Global Monsoon Model Intercomparison Project (GMMIP; Zhou et al., 2016). Past changes, simulation and attribution, and projections of the GM are assessed in Sections 2.3.1.4.2, 3.3.3.2 and 4.4.1.4, respectively.

[START Figure AV.1 HERE]

Figure AV.1: Global and regional monsoons domains. AR6 global monsoon area is represented by the black contour. AR6 regional monsoons are: North American monsoon (shaded magenta), South American monsoon (shaded dark-orange), West African monsoon (shaded grey), South and Southeast Asian monsoon (shaded pink), East Asian monsoon (shaded purple) and Australian-Maritime Continent monsoon (shaded yellow). Areas over Equatorial America and South Africa (dotted red and magenta, respectively) are highlighted but not identified as specific regional monsoons (see explanation in the main text). For each regional monsoon, the seasonal characteristics associated with each domain are specified in the main text.

[END Figure AV.1 HERE]

AV.3 Rationale for regional monsoons definitions in AR6

The definition of the regional monsoons has been slightly modified in AR6 with respect to AR5, starting from the consideration that some of the continental areas identified using the global metric have a seasonality in precipitation that is not necessarily of monsoon origin. In particular, the dotted regions in Figure AV.1 located over South Africa, Central America and equatorial South America have a strong seasonality in precipitation but their qualification as monsoons is a subject of discussion. In the assessment of the regional monsoons in Sections 8.3.2.4 and 8.4.2.4, these regions are not considered as distinct regional monsoons, but they are discussed in Box 8.2 that is dedicated to changes in water cycle seasonality. The domains of the regional monsoons in AR6 are defined based on published literature and expert judgement, and accounting for the fact that the climatological summer monsoon rainy season varies across the individual monsoon regions. As shown in Figure AV.1, AR6 regional monsoons are: South and Southeast Asian (Section AV.4.1), East Asian (Section AV.4.2), West African (Section AV.4.3), North American (Section AV.4.4), South American (Section AV.4.5) and Australian-Maritime Continent (Section AV.4.6). For each region the definition, regional justification and key features are provided, along with cross references to the main areas of assessment in AR6.

AV.4 Definition of regional monsoons

AV.4.1 The South and Southeast Asian monsoon

The South and Southeast Asian monsoon (SAsiaM) is characterized by pronounced seasonal reversal of wind and precipitation. It covers vast geographical areas and several countries including India, Bangladesh, Nepal, Myanmar, Sri Lanka, Pakistan, Thailand, Laos, Cambodia, Vietnam and the Philippines (Pant and Rupa Kumar, 1997; Goswami, 2006; Gadgil et al., 2010; Shige et al., 2017), with a domain roughly extending across 60°-110°E and 10°S-25°N as shown in Figure AV.1 (shaded pink). The SAsiaM is unique in its geographical features because of the orography surrounding the area (i.e., the Himalayas, Western Ghats and Arakan Yoma mountains, and Tibetan Plateau to the north) and the adjacent Indian Ocean.

The SAsiaM rainy season from June to September contributes to more than 75% of the annual rainfall over much of the region, including the southern slopes of the central and eastern Himalayas (Krishnan et al., 2019b). Considering the spatial domain of the SAsiaM, monsoon precipitation maxima are located over the west coast, northeast and central north India, Myanmar and Bangladesh, whereas minima are located over northwest and south-eastern India, western Pakistan, and south-eastern and northern Sri Lanka (Pant and Rupa Kumar, 1997; Gadgil et al., 2010). Prior to the SAsiaM rainy season, areas in the north-western Himalaya receive precipitation during winter and early spring from so-called “western disturbances”, which are extratropical synoptic systems originating over the Mediterranean region and propagating eastward along the sub-tropical westerly jet (Madhura et al., 2014; Cannon et al., 2015; Dimri et al., 2015; Hunt et al., 2018; Krishnan et al., 2019a, 2019b).

The climatological onset of the SAsiaM occurs around 20 May over the Andaman and Nicobar Islands and covers the central Bay of Bengal around 25 May, while it simultaneously advances into mainland India from the south through Kerala (Pai et al., 2020). The normal date of monsoon onset over Kerala is 1 June and the monsoon rains progress into India both from south to north and east to west, so as to cover the entire country by 15 July (Pai et al., 2020), although with large interannual and interdecadal variations (Ghanekar et al., 2019). Retreat of the SAsiaM typically begins from far northwest India around 1 September and withdraws completely from the country by 15 October; this is followed by establishment of the northeast monsoon rainy season over south peninsular India from October through December (Pai et al., 2020).

The SAsiaM exhibits prominent rainfall variability on subseasonal, interannual and interdecadal time scales with teleconnections to modes of climate variability (see Webster et al., 1998; Turner and Annamalai, 2012). While the gross features of the SAsiaM are simulated in GCMs, there are several large biases that have persisted over generations of climate models, in CMIP3 and CMIP5, including a large dry bias over India coupled to a lower-tropospheric circulation that is too weak (Sperber et al., 2013) and a related wet bias over the western equatorial Indian Ocean (Bollasina and Ming, 2013). In CMIP5, cold Arabian Sea SST biases in coupled GCMs were shown to worsen the monsoon dry bias by limiting the available moisture (Levine et al., 2013; Sandeep and Ajayamohan, 2015). Some improvements to the spatial pattern have been noted in CMIP6, particularly near orography (Gusain et al., 2020). The teleconnection to the El Niño-Southern Oscillation (ENSO) provides the main prospect for seasonal prediction and was too weak in CMIP5 (Sperber et al., 2013). The boreal summer intraseasonal oscillation (BSISO) controls the majority of subseasonal variations in SAsiaM rainfall, as well as affecting the East Asian monsoon region. While CMIP5 models better represented the BSISO than CMIP3 (especially its characteristic northward propagation), the spatial pattern is still poorly simulated in most models (Sabeerali et al., 2013).

The SAsiaM is assessed in Sections 8.3.2.4.1, 8.4.2.4.1, Atlas.5.3.2 and Atlas.5.3.4. One of its main components, the Indian summer monsoon, is assessed in Section 10.6.3 as a case study on the construction of regional climate information from the distillation of multiple lines of evidence. Climate change over the Hindu Kush-Himalaya is assessed in CCB10.4.

AV.4.2 The East Asian monsoon

The East Asian monsoon (EAsiaM) is the seasonal reversal in wind and precipitation occurring over East Asia, including eastern China, Japan and the Korean Peninsula. The continental area influenced by this monsoon is roughly bounded by 102.5°-140°E and 20°-40°N (e.g., Wen et al., 2000; Wang and LinHo, 2002; Wang et al., 2010), and is shaded purple in Figure AV.1. Unlike other monsoons, it extends quite far north, out of the tropical belt, and it is largely influenced by subtropical systems, such as the Western North Pacific subtropical high, East Asian subtropical westerly jet, and by disturbances from the mid-latitudes (Chang et al., 2000; Lee et al., 2006, 2013b; Yim et al., 2008; Zhou et al., 2009).

The EAsiaM manifests during boreal summer with warm and wet southerly winds, but also during boreal winter with cold and dry northerly winds (Ha et al., 2012). The winter component has been linked to the subsequent summer (i.e., Wen et al., 2000, 2016; Ge et al., 2017; Yan et al., 2020).

AV.4.2.1 The summer EAsiaM

The summer EAsiaM is a subtropical monsoon system (e.g., Wang and LinHo, 2002; Ding et al., 2007). It is characterized by low-level southerly winds prevailing over eastern China, Korea and Japan in boreal summer. The monsoon flow brings abundant water vapour into East Asia that converges and forms the Meiyu/Baiu/Changma rain belt over the region (Zhou et al., 2009; Jin et al., 2013; Lee et al., 2017). In late April/early May, rainfall onsets in central Indochina Peninsula, and in mid-June the rainy season arrives over East Asia with the formation of the Meiyu front along the Yangtze River valley, Changma in Korea and Baiu in Japan. Later in July, the monsoon advances up to North China, the Korean peninsula and central Japan (Zhang et al., 2004; Yihui and Chan, 2005; Zhou et al., 2009).

Intraseasonal variability of the EAsiaM has been mostly related to the Madden Julian Oscillation (MJO) (Yasunari, 1979; Zhang et al., 2009; Chen et al., 2015), to the phase of the Pacific-Japan mode (Nitta, 1987) or the Indian summer monsoon (Li et al., 2018) and to the BSISO (Kikuchi et al., 2012; Chen et al., 2015), particularly for its onset (Lee et al., 2013a). At interannual time scales, changes in summer EAsiaM intensity lead to a position shift of the monsoon rain belt under the influence of ENSO (Wang et al., 2000) and the western Pacific subtropical high (Kosaka et al., 2013; Wang et al., 2013), Arctic sea ice (Guo et al., 2014) and solar and volcanic forcing (Peng et al., 2010; Man et al., 2012; Cui et al., 2014). Variability at interdecadal timescale is more prominent in the second half of the 20th century (Jiang, 2005; Ding et al., 2008; Wang et al., 2018), and a specific assessment about this aspect is provided in Section 8.3.2.4.2.

The basic features and interannual variations of the summer EAsiaM are well reproduced in climate models. For example, the climatological circulation structure is well reproduced in both atmospheric and coupled GCMs (Song and Zhou, 2013; Song et al., 2013; Jiang et al., 2016, 2020), and the relationship between the monsoon and ENSO is well represented (Sperber et al., 2013; Fu and Lu, 2017). In CMIP5 models, the main shortcomings relate to missing rainfall bands around 30°N and the northward shift of the western North Pacific subtropical high (Huang et al., 2013). Most coupled models show an inadequate strength of monsoon circulation over southern East Asia, and with little change in model performance from the TAR to AR6 (Jiang et al., 2016, 2020). In coupled model simulations, air-sea coupling helps improve the climatology and interannual variability of rainfall over the East Asia monsoon region (Wang, 2005; Song and Zhou, 2014).

The summer (June-July-August) component of the EAsiaM is assessed in Sections 8.3.2.4.2, 8.4.2.4.2, Atlas.5.1.2 and Atlas.5.1.4.

AV.4.2.2 The winter EAsiaM

The winter EAsiaM is characterized by strong north-westerlies over northeast China, Korea and Japan, and by strong north-easterlies along the coast of East Asia (Huang et al., 2003). The northerly wind extends from midlatitude East Asia to the equatorial South China Sea (Wen et al., 2000; Wang et al., 2010). The winter EAsiaM has one component mostly linked to mid-to-high latitude circulation systems and another mostly linked to the tropical circulation and largely controlled by ENSO (Ge et al., 2012; Chen et al., 2014a). The mid-latitude component has a close relationship with autumn Arctic sea-ice concentration changes (Chen et al., 2014b).

The winter EAsiaM exhibits significant variability ranging from intra-seasonal to interdecadal timescales. Its intra-seasonal variability is suggested to be influenced by both high-latitude and subtropical Eurasian wave trains (Jiao et al., 2019). At the interannual timescale, ENSO is an important factor modulating the winter EAsiaM (Wang et al., 2000), while the relationship between them is not stable (Wang and He, 2012; Fan et al., 2020). In addition, Arctic Oscillation (Gong et al., 2001), Arctic sea ice (Ge et al., 2012), Eurasian snow (Luo and Wang, 2019), and strong volcanic eruptions (Miao et al., 2016) also play vital roles in changing the winter EAsiaM intensity. At the interdecadal timescale, the winter EAsiaM weakened significantly in the mid-1980s, which resulted from atmospheric intrinsic quasi-stationary planetary waves (Wang et al., 2009) and external forcings (Miao et al., 2018). In the mid-2000s, the winter EAsiaM was observed to recover from its weak epoch (Wang and Chen, 2014).

The large-scale features of the winter EAsiaM are well reproduced by climate models, although the strength of monsoon circulation is underestimated. The ability of coupled models to simulate the winter EAsiaM shows little difference through the TAR to AR5, but has improved from AR5 to AR6 (Jiang et al., 2016, 2020). In CMIP5 models, reasonable simulations of the Siberian high and Aleutian low intensities and the ENSO-winter EAsiaM relationship help improve the climatology and interannual variability of the winter EAsiaM (Gong et al., 2014).

Model simulations of the winter component of the EAsiaM are assessed in chapter Atlas.5.1.3.

AV.4.3 The West African Monsoon

The West African monsoon (WAfriM) is a seasonal reversal in wind and precipitation extending over a vast and contrasted geographical region, from the Equator to the margins of the Sahara, and from the Atlantic coast inland. The WAfriM domain includes Togo, Guinea Bissau, Gambia, Senegal, Mauritania, Guinea, Sierra Leone, Liberia, Mali, Ivory Coast, Burkina Faso, Ghana, Benin, Chad, Cape Verde, northern Cameroon, Niger, Nigeria and northern Central African Republic. It can thus be roughly bounded by 18°W-30°E, 5°-18°N and is grey shaded in Figure AV.1 (e.g., Adedokun, 1978). The West African monsoon and Sahel are sometimes considered interchangeably. However, the Sahel lies in the northern part of the WAfriM region, often limited to the west and central north Africa (e.g., Nicholson et al. (2018) considered the domain to be 20°W-30°E, 10°-20°N) or sometimes extended to the east (e.g., Giannini and Kaplan (2019) considered the domain to be 20°W-40°E, 10°-20°N). The East African region with the Greater Horn of Africa, which includes Ethiopia, Sudan, and South Sudan, lies on the fringes of both the West African and Indian monsoons (Nicholson, 2017).

The WAfriM is characterized by the northward progression from May to September of moist low-level south-westerlies from the Gulf of Guinea, meeting the dry north-easterlies (Harmattan) from the Saharan heat low at the intertropical discontinuity (e.g., Hamilton et al., 1945; Omotosho, 1988). In May and June, rainfall remains essentially along the Guinean coast with a maximum occurring near 5°N, then the rainfall maximum jumps suddenly over the Sudan-Sahel zone near 12°N, followed by a "little dry season" over the Guinea coast (Adejuwon and Odekunle, 2006). This apparent shift is known as the West African monsoon jump and it is concomitant with the monsoon onset over the Sahel (Sultan and Janicot, 2003; Cook, 2015). Rainfall continues to progress towards the north up to about 18-20°N. The rainfall maximum occurs in the Sahel in August/September, followed by a rapid retreat of rainfall to the Guinean Coast and a second maximum occurs over this region in October/November.

The WAfriM features variability at different timescales. Unprecedent droughts occurred in West Africa and particularly over the Sahel from the late 1960s to the mid-1990s, and a specific assessment of the understanding of mechanisms related to these changes is provided in Sections 8.3.2.4.3 and 10.4.2.1.

At interannual time scales, tropical oceans (Atlantic, Pacific and Indian) appear to be the major drivers with their SSTs anomalies leading to variations in the accumulated seasonal rainfall (e.g., Lamb, 1978; Diakhate et al, 2019). At intraseasonal time scales, equatorial waves (e.g., Mekonnen et al., 2008; Janicot et al., 2010) and interactions with mid-latitudes and the Mediterranean (e.g., Vizy and Cook, 2009; Roehrig et al., 2011) have an effect on WAfriM activity. African Easterly Waves (AEWs) and mesoscale convective systems (MCSs), including squall lines, are the prominent weather synoptic scale aspects of the WAfriM, supplying almost all rainfall in the Sahel. The strong coupling between AEWs and MCSs has been investigated in depth, as well as their interactions with the Saharan Heat Low, the moisture supply from East Africa and the Mediterranean region or from near the equator (e.g., Diongue et al., 2002; Brammer and Thorncroft, 2017; Lafore et al., 2017). Land surface processes are known to influence WAfriM precipitation (Boone et al., 2016).

Simulation of West Africa climate, including the monsoon, has received specific attention under coordinated programmes in the recent past: the African Multidisciplinary Monsoon Analysis Model Intercomparison Project (AMMA-MIP), the AMMA Land-surface Model Intercomparison Project (ALMIP), the West African Monsoon Modelling and Evaluation (WAMME) project and the Coordinated Regional Downscaling Experiment (CORDEX) (Raj et al., 2019). CMIP5 and CMIP6 struggle to reproduce the amplitude of observed decadal variability in the twenty century and to represent the mean climatology including the northward propagation of the monsoon (Roehrig et al., 2013; Monerie et al., 2020; Sow et al., 2020). A higher horizontal resolution improves the representation of the intensity and spatial distribution of WAfriM rainfall and related circulation, because of the effects of vegetation, orography and coastlines (Hourdin et al., 2010; Sylla et al., 2010; Xue et al., 2010; Raj et al., 2019).

The WAfriM is assessed in Sections 8.3.2.4.3 and 8.4.2.4.3. The observed Sahel and West African monsoon drought and recovery is assessed as a regional climate change attribution example in Section 10.4.2.1.

AV.4.4 The North American Monsoon

The North American monsoon (NAmerM) is a regional-scale atmospheric circulation system dominated by boreal summer precipitation over northwestern Mexico and southwest United States, where it contributes to almost 70% and 40% of the total annual precipitation, respectively (Douglas et al., 1993; Higgins et al., 1997). The NAmerM domain is shaded magenta in Figure AV.1, roughly bounded by 15°-35°N, 100°-115°W and defined where the July-August-September minus June mean precipitation exceeds 25mm/mon (Douglas et al., 1993; Adams and Comrie, 1997; Barlow et al., 1998; Cook and Seager, 2013).

The identification of a regional monsoon regime in North America dates back to the 1990s (Douglas et al., 1993; Adams and Comrie, 1997; Higgins et al., 1997; Barlow et al., 1998), although consideration of the monsoonal character of the southwestern United States precipitation goes back considerably further (e.g., Bryson and Lowry, 1955). The monsoonal characteristics of the region include a pronounced annual maximum of precipitation in boreal summer (June-July-August) accompanied by a surface low pressure system and an upper-level anticyclone, although the seasonal reversal of the surface winds is primarily limited to the northern Gulf of California. In particular, the summertime precipitation in the NAmerM region is dictated by the location of the upper-level anticyclone (Reed, 1933; Castro et al., 2001). The decay phase of the NAmerM is typically observed during late September-October, when convection migrates from Central to South America (Vera et al., 2006).

Mesoscale variability of the NAmerM comes from the pulsing of the Gulf of California low-level jet, the intensification/reduction of the land-sea contrast (Torres-Alavez et al., 2014) and moisture surges over the Gulf of California (Vera et al., 2006). Synoptic variability of the NAmerM is mainly associated with the activity of tropical cyclones and of easterly waves (Stensrud et al., 1997; Fuller and Stensrud, 2000). In addition, the NAmerM is strongly influenced by the ENSO variability at both the interannual (Higgins et al., 1999; Higgins and Shi, 2001) and decadal (e.g., Castro et al., 2001) time scales.

The region is challenging for climate modeling for several reasons, including complex topography, importance of Mesoscale Convective Systems (MCSs), and sensitivity to SST bias (e.g., Pascale et al., 2019). Many CMIP3 and CMIP5 models with resolutions coarser than 100 km are unable to realistically resolve the topography of the NAmerM region, thus inducing biases in simulating the monsoon (Geil et al., 2013). Among other factors, these biases are due to biases in the simulation of the Gulf of California summertime low-level flow (Kim et al., 2008; Pascale et al., 2017) and to failures in representing properly the diurnal cycle (Risanto et al., 2019) and the decay (Bukovsky et al., 2015) of the NAmerM precipitation. Simulations at higher horizontal resolution (i.e. with at least 0.25º grid) exhibit an improved representation of the regional topography, which provides a better representation of the regional circulation and therefore of the NAmerM (Varuolo-Clarke et al., 2019).

The NAmerM is assessed in Sections 8.3.2.4.4 and 8.4.2.4.4.

AV.4.5 The South American Monsoon

The South American monsoon (SAmerM) is a regional circulation system characterized by inflow of low-level winds from the Atlantic Ocean toward South America, involving Brazil, Perù, Bolivia and northern Argentina, associated with the development of surface pressure gradients (and intense precipitation) during austral summer (December-January-February). Based on climatological precipitation intensity, the SAmerM region is roughly bounded by 5°-25°S and 70°-50°W (Zhou and Lau, 1998; Vera et al., 2006; Raia and Cavalcanti, 2008) and is dark-orange shaded in Figure AV.1.

During austral spring (September-October-November), areas of intense convection migrate from northwestern South America to the south (Raia and Cavalcanti, 2008), forming the South Atlantic Convergence Zone (SACZ) during austral summer (Kodama, 1992; Jones and Carvalho, 2002; Vera et al., 2006). Associated with this regime, an upper-tropospheric anticyclone (the Bolivian High) forms over the Altiplano region during the monsoon onset (Lenters and Cook, 1997). The establishment of this upper-level anticyclone has been related to the transition from southerly to northerly winds and the occurrence of strong convective heating over the Amazon (Lenters and Cook, 1997; Wang and Fu, 2002). The SAmerM then retreats during austral autumn/fall (March-April-May) with a northeastward migration of the convection (e.g., Vera et al., 2006).

The SAmerM displays considerable variability on time scales raging from intraseasonal to decadal (Vera et al., 2006; Marengo et al., 2012; Vuille et al., 2012; Novello et al., 2017). The Madden-Julian Oscillation (MJO, Section AVI.2.8) influences the SACZ via changes in midlatitude synoptic disturbances (Jones and

Carvalho, 2002; Liebmann et al., 2004). At interannual time scales, ENSO explains most of the SAmerM variability (e.g., Paegle and Mo, 2002; Marengo et al., 2012).Tropical Atlantic temperatures also affect the SAmerM, with reduced atmospheric moisture transport to feed the monsoon under a warmer tropical north Atlantic conditions (e.g., Marengo et al., 2008; Zeng et al., 2008). In addition to SSTs, interannual variability of the SAmerM is linked to changes in land surface processes, cold-air incursions, the latitudinal location of the subtropical jet, and the Southern Annular Mode (Section AVI.2.2) (e.g., Silvestri, 2003; Li and Fu, 2004; Collini et al., 2008; Yin et al., 2014). At interdecadal timescales, the SAmerM is influenced by important modes of climate variability (e.g., Robertson and Mechoso, 2000; Paegle and Mo, 2002; Chiessi et al., 2009; Silvestri and Vera, 2009).

The general large-scale features of the SAmerM are reasonably well simulated by coupled climate models although they do not adequately reproduce maximum precipitation over the core of the monsoon, even when considering simulations under past natural forcings, such as those during the last millennium (Rojas et al., 2016; Díaz and Vera, 2018). However, CMIP5 models featured an improved representation of the SAmerM with respect to CMIP3 (Joetzjer et al., 2013; Jones and Carvalho, 2013; Gulizia and Camilloni, 2015; Díaz and Vera, 2017).

The SAmerM is assessed in Sections 8.3.2.4.5 and 8.4.2.4.5.

AV.4.6 The Australian-Maritime Continent monsoon

The Australian-Maritime Continent monsoon (AusMCM) occurs during austral summer (December-January-February), with the large-scale shift of the Inter-Tropical Convergence Zone into the Southern Hemisphere. It covers northern Australia and the Maritime Continent up to 10°N (e.g., McBride, 1987; Suppiah, 1992; Robertson et al., 2011), and it corresponds to the yellow shaded region in Figure AV.1. The identification of the Australian monsoon by meteorologists dates back to the early 20th century (see review of Suppiah, 1992), with later studies providing classifications of monsoon circulation regimes (e.g., McBride, 1987) and definitions of monsoon onset (Troup, 1961; Holland, 1986; Hendon and Liebmann, 1990; Drosdowsky, 1996).

The AusMCM is characterized by the seasonal reversal of prevailing easterly winds to westerly winds and the onset of periods of active convection and heavy rainfall (Zhang and Moise, 2016). Over northern Australia, the monsoon season generally lasts from December to March and is associated with west to northwesterly inflow of moist winds, producing convection and heavy precipitation. Over the Maritime Continent, the main rainy season south of the equator is centered on December to February with northwesterly monsoon flow at low levels.

Over Australia, the monsoon is strongly influenced by ENSO on interannual timescales: during El Niño years the monsoon onset tends to be delayed (Nicholls et al., 1982; McBride and Nicholls, 1983; Drosdowsky, 1996). This relationship breaks down after the onset of the wet season, leading to little correlation between ENSO phase and total monsoon rainfall or duration (e.g., Hendon et al., 2012). The Maritime Continent also experiences a delay in monsoon onset during El Niño years and monsoon rainfall is correlated with ENSO during the dry and transition seasons (Robertson et al., 2011). The AusMCM is also influenced by the Indian Ocean Dipole (peaking in September -November) that tends to weaken the following monsoon when in its positive phase (Cai et al., 2005).

The ability of climate models to simulate the Australian monsoon has improved in successive generations of coupled models (i.e., from CMIP3 to CMIP6, Moise et al., 2012; Brown et al., 2016; Narsey et al., 2020), with sensitivity of monsoon rainfall to the magnitude of SST biases in the equatorial Pacific (Brown et al., 2016).

The AusMCM is assessed in Sections 8.3.2.4.6 and 8.4.2.4.6.

References

Adams, D. K., and Comrie, A. C. (1997). The North American Monsoon. *Bull. Am. Meteorol. Soc.* 78, 2197–2213. doi:10.1175/1520-0477(1997)078<2197:TNAM>2.0.CO;2.

Adedokun, J. A. (1978). West African precipitation and dominant atmospheric mechanisms. *Arch. für Meteorol. Geophys. und Bioklimatologie Ser. A* 27, 289–310. doi:10.1007/BF02247952.

Adejuwon, J. O., and Odekunle, T. O. (2006). Variability and the Severity of the "Little Dry Season" in Southwestern Nigeria. *J. Clim.* 19, 483–493. doi:10.1175/JCLI3642.1.

An, Z., Wu, G., Li, J., Sun, Y., Liu, Y., Zhou, W., et al. (2015). Global Monsoon Dynamics and Climate Change. *Annu. Rev. Earth Planet. Sci.* 43, 29–77. doi:10.1146/annurev-earth-060313-054623.

Barlow, M., Nigam, S., and Berbery, E. H. (1998). Evolution of the North American monsoon system. *J. Clim.* 11, 2238–2257. doi:10.1175/1520-0442(1998)011<2238:EOTNAM>2.0.CO;2.

Biasutti, M., Voigt, A., Boos, W. R., Braconnot, P., Hargreaves, J. C., Harrison, S. P., et al. (2018). Global energetics and local physics as drivers of past, present and future monsoons. *Nat. Geosci.* 11, 392–400. doi:10.1038/s41561-018-0137-1.

Bollasina, M. A., and Ming, Y. (2013). The general circulation model precipitation bias over the southwestern equatorial Indian Ocean and its implications for simulating the South Asian monsoon. *Clim. Dyn.* 40, 823–838. doi:10.1007/s00382-012-1347-7.

Boone, A. A., Xue, Y., De Sales, F., Comer, R. E., Hagos, S., Mahanama, S., et al. (2016). The regional impact of Land-Use Land-cover Change (LULCC) over West Africa from an ensemble of global climate models under the auspices of the WAMME2 project. *Clim. Dyn.* 47, 3547–3573. doi:10.1007/s00382-016-3252-y.

Brammer, A., and Thorncroft, C. D. (2017). Spatial and Temporal Variability of the Three-Dimensional Flow around African Easterly Waves. *Mon. Weather Rev.* 145, 2879–2895. doi:10.1175/MWR-D-16-0454.1.

Brown, J. R., Moise, A. F., Colman, R., and Zhang, H. (2016). Will a Warmer World Mean a Wetter or Drier Australian Monsoon? *J. Clim.* 29, 4577–4596. doi:10.1175/JCLI-D-15-0695.1.

Bryson, R., and Lowry, W. (1955). Synoptic climatology of the Arizona summer monsoon.

Bukovsky, M. S., Carrillo, C. M., Gochis, D. J., Hammerling, D. M., McCrary, R. R., and Mearns, L. O. (2015). Toward assessing NARCCAP regional climate model credibility for the North American monsoon: Future climate simulations. *J. Clim.* 28, 6707–6728. doi:10.1175/JCLI-D-14-00695.1.

Cai, W., Hendon, H. H., and Meyers, G. (2005). Indian Ocean Dipolelike Variability in the CSIRO Mark 3 Coupled Climate Model. *J. Clim.* 18, 1449–1468. doi:10.1175/JCLI3332.1.

Cannon, F., Carvalho, L. M. V., Jones, C., and Bookhagen, B. (2015). Multi-annual variations in winter westerly disturbance activity affecting the Himalaya. *Clim. Dyn.* 44, 441–455. doi:10.1007/s00382-014-2248-8.

Castro, C. L., McKee, T. B., and Pielke, R. A. (2001). The relationship of the North American Monsoon to tropical and North Pacific Sea surface temperatures as revealed by observational analyses. *J. Clim.* 14, 4449–4473. doi:10.1175/1520-0442(2001)014<4449:TROTNA>2.0.CO;2.

Chang, C.-P., Zhang, Y., and Li, T. (2000). Interannual and Interdecadal Variations of the East Asian Summer Monsoon and Tropical Pacific SSTs. Part I: Roles of the Subtropical Ridge. *J. Clim.* 13, 4310–4325. doi:10.1175/1520-0442(2000)013<4310:IAIVOT>2.0.CO;2.

Chen, J., Wen, Z., Wu, R., Chen, Z., and Zhao, P. (2015). Influences of northward propagating 25–90-day and quasi-biweekly oscillations on eastern China summer rainfall. *Clim. Dyn.* 45, 105–124. doi:10.1007/s00382-014-2334-y.

Chen, Z., Wu, R., and Chen, W. (2014a). Distinguishing Interannual Variations of the Northern and Southern Modes of the East Asian Winter Monsoon. *J. Clim.* 27, 835–851. doi:10.1175/JCLI-D-13-00314.1.

Chen, Z., Wu, R., and Chen, W. (2014b). Impacts of Autumn Arctic Sea Ice Concentration Changes on the East Asian Winter Monsoon Variability. *J. Clim.* 27, 5433–5450. doi:10.1175/JCLI-D-13-00731.1.

Chiessi, C. M., Mulitza, S., Pätzold, J., Wefer, G., and Marengo, J. A. (2009). Possible impact of the Atlantic Multidecadal Oscillation on the South American summer monsoon. *Geophys. Res. Lett.* 36, L21707. doi:10.1029/2009GL039914.

Collini, E. A., Berbery, E. H., Barros, V. R., and Pyle, M. E. (2008). How Does Soil Moisture Influence the Early Stages of the South American Monsoon? *J. Clim.* 21, 195–213. doi:10.1175/2007JCLI1846.1.

Cook, B. I., and Seager, R. (2013). The response of the North American Monsoon to increased greenhouse gas forcing. *J. Geophys. Res. Atmos.* 118, 1690–1699. doi:10.1002/jgrd.50111.

Cook, K. H. (2015). Role of inertial instability in the West African monsoon jump. *J. Geophys. Res. Atmos.* 120, 3085–3102. doi:10.1002/2014JD022579.

Cui, X., Gao, Y., and Sun, J. (2014). The response of the East Asian summer monsoon to strong tropical volcanic eruptions. *Adv. Atmos. Sci.* 31, 1245–1255. doi:10.1007/s00376-014-3239-8.

Diakhaté, M., Rodríguez-Fonseca, B., Gómara, I., Mohino, E., Dieng, A. L., and Gaye, A. T. (2019). Oceanic Forcing on Interannual Variability of Sahel Heavy and Moderate Daily Rainfall. *J. Hydrometeorol.* 20, 397–410. doi:10.1175/JHM-D-18-0035.1.

Díaz, L. B., and Vera, C. S. (2017). Austral summer precipitation interannual variability and trends over Southeastern South America in CMIP5 models. *Internatio*, 1–15. doi:10.1002/joc.5031.

Díaz, L. B., and Vera, C. S. (2018). South American precipitation changes simulated by PMIP3/CMIP5 models during the Little Ice Age and the recent global warming period. *Int. J. Climatol.* 38, 2638–2650. doi:10.1002/joc.5449.

Dimri, A. P., Niyogi, D., Barros, A. P., Ridley, J., Mohanty, U. C., Yasunari, T., et al. (2015). Western Disturbances: A review. *Rev. Geophys.* 53, 225–246. doi:10.1002/2014RG000460.

Ding, Y., Ren, G., Zhao, Z., Xu, Y., Luo, Y., Li, Q., et al. (2007). Detection, causes and projection of climate change over China: An overview of recent progress. *Adv. Atmos. Sci.* 24, 954–971. doi:10.1007/s00376-007-0954-4.

Ding, Y., Wang, Z., and Sun, Y. (2008). Inter-decadal variation of the summer precipitation in East China and its association with decreasing Asian summer monsoon. Part I: Observed evidences. *Int. J. Climatol.* 28, 1139–1161. doi:10.1002/joc.1615.

Diongue, A., Lafore, J.-P., Redelsperger, J.-L., and Roca, R. (2002). Numerical study of a Sahelian synoptic weather system: Initiation and mature stages of convection and its interactions with the large-scale dynamics. *Q. J. R. Meteorol. Soc.* 128, 1899–1927. doi:10.1256/003590002320603467.

Douglas, M. W., Maddox, R. A., Howard, K., and Reyes, S. (1993). The Mexican monsoon. *J. Clim.* 6, 1665–1677. doi:10.1175/1520-0442(1993)006<1665:TMM>2.0.CO;2.

Drosdowsky, W. (1996). Variability of the Australian Summer Monsoon at Darwin: 1957–1992. *J. Clim.* 9, 85–96. doi:10.1175/1520-0442(1996)009<0085:VOTASM>2.0.CO;2.

Fan, G., Lv, F., Zhang, J., and Fu, J. (2020). A possible way to extract a stationary relationship between ENSO and the East Asian winter monsoon. *Atmos. Ocean. Sci. Lett.* 13, 294–300. doi:10.1080/16742834.2020.1733918.

Fu, Y., and Lu, R. (2017). Improvements in Simulating the Relationship between ENSO and East Asian Summer Rainfall in the CMIP5 Models. *J. Clim.* 30, 4513–4525. doi:10.1175/JCLI-D-16-0606.1.

Fuller, R. D., and Stensrud, D. J. (2000). The Relationship between Tropical Easterly Waves and Surges over the Gulf of California during the North American Monsoon. *Mon. Weather Rev.* 128, 2983–2989. doi:10.1175/1520-0493(2000)128<2983:TRBTEW>2.0.CO;2.

Gadgil, S., Rajeevan, M., Zubair, L., and Yadav, P. (2010). "Interannual variations of the South Asian monsoon: Links with ENSO and EQUINOO," in *The Global Monsoon System - Research and Forecast*, eds. C.-P. Chang, Y. Ding, N.-C. Lau, H. R. Johnson, B. Wang, and T. Yasunari (World Scientific).

Ge, L., Li-Ren, J., Shu-Qing, S., and Yu-Fei, X. (2012). Low- and Mid-High Latitude Components of the East Asian Winter Monsoon and Their Reflecting Variations in Winter Climate over Eastern China. *Atmos. Ocean. Sci. Lett.* 5, 195–200. doi:10.1080/16742834.2012.11446985.

Ge, Q., Xue, Z., Yao, Z., Zang, Z., and Chu, F. (2017). Anti-phase relationship between the East Asian winter monsoon and summer monsoon during the Holocene? *J. Ocean Univ. China* 16, 175–183. doi:10.1007/s11802-017-3098-x.

Geen, R., Bordoni, S., Battisti, D. S., and Hui, K. (2020). Monsoons, ITCZs and the Concept of the Global Monsoon. *Rev. Geophys.* n/a, e2020RG000700. doi:https://doi.org/10.1029/2020RG000700.

Geil, K. L., Serra, Y. L., and Zeng, X. (2013). Assessment of CMIP5 model simulations of the North American monsoon system. *J. Clim.* doi:10.1175/JCLI-D-13-00044.1.

Ghanekar, S. P., Bansod, S. D., Narkhedkar, S. G., and Kulkarni, A. (2019). Variability of Indian summer monsoon onset over Kerala during 1971–2018. *Theor. Appl. Climatol.* 138, 729–742. doi:10.1007/s00704-019-02853-5.

Giannini, A., and Kaplan, A. (2019). The role of aerosols and greenhouse gases in Sahel drought and recovery. *Clim. Change* 152, 449–466. doi:10.1007/s10584-018-2341-9.

Gong, D.-Y., Wang, S.-W., and Zhu, J.-H. (2001). East Asian Winter Monsoon and Arctic Oscillation. *Geophys. Res. Lett.* 28, 2073–2076. doi:10.1029/2000GL012311.

Gong, H., Wang, L., Chen, W., Wu, R., Wei, K., and Cui, X. (2014). The Climatology and Interannual Variability of the East Asian Winter Monsoon in CMIP5 Models. *J. Clim.* 27, 1659–1678. doi:10.1175/JCLI-D-13-00039.1.

Goswami, B. N. (2006). "Intraseasonal variability in the atmosphere-ocean climate system," in *South Asian Monsoon*, eds. W. K. M. Lau and D. E. Waliser (Springer Praxis), 19–55.

Gulizia, C., and Camilloni, I. (2015). Comparative analysis of the ability of a set of CMIP3 and CMIP5 global climate models to represent precipitation in South America. *Int. J. Climatol.* 35, 583–595. doi:https://doi.org/10.1002/joc.4005.

Guo, D., Gao, Y., Bethke, I., Gong, D., Johannessen, O. M., and Wang, H. (2014). Mechanism on how the spring Arctic sea ice impacts the East Asian summer monsoon. *Theor. Appl. Climatol.* 115, 107–119. doi:10.1007/s00704-013-0872-6.

Gusain, A., Ghosh, S., and Karmakar, S. (2020). Added value of CMIP6 over CMIP5 models in simulating Indian summer monsoon rainfall. *Atmos. Res.* 232, 104680. doi:10.1016/j.atmosres.2019.104680.

Ha, K.-J., Heo, K.-Y., Lee, S.-S., Yun, K.-S., and Jhun, J.-G. (2012). Variability in the East Asian Monsoon: a review. *Meteorol. Appl.* 19, 200–215. doi:10.1002/met.1320.

Hamilton, R. A., Archbold, J. W., and Douglas, C. K. M. (1945). Meteorology of Nigeria and adjacent territory. *Q. J. R. Meteorol. Soc.* 71, 231–264. doi:10.1002/qj.49707130905.

Hendon, H. H., and Liebmann, B. (1990). A Composite Study of Onset of the Australian Summer Monsoon. *J. Atmos. Sci.* 47, 2227–2240. doi:10.1175/1520-0469(1990)047<2227:ACSOOO>2.0.CO;2.

Hendon, H. H., Lim, E.-P., and Liu, G. (2012). The Role of Air–Sea Interaction for Prediction of Australian Summer Monsoon Rainfall. *J. Clim.* 25, 1278–1290. doi:10.1175/JCLI-D-11-00125.1.

Higgins, R. W., Chen, Y., and Douglas, A. V. (1999). Interannual variability of the North American warm season precipitation regime. *J. Clim.* 12, 653–680. doi:10.1175/1520-0442(1999)012<0653:ivotna>2.0.co;2.

Higgins, R. W., and Shi, W. (2001). Intercomparison of the Principal Modes of Interannual and Intraseasonal Variability of the North American Monsoon System. *J. Clim.* 14, 403–417. Available at: http://www.jstor.org/stable/26247310.

Higgins, R. W., Yao, Y., and Wang, X. L. (1997). Influence of the North American monsoon system on the U.S. summer precipitation regime. *J. Clim.* 10, 2600–2622. doi:10.1175/1520-0442(1997)010<2600:IOTNAM>2.0.CO;2.

Holland, G. J. (1986). Interannual Variability of the Australian Summer Monsoon at Darwin: 1952–82. *Mon. Weather Rev.* 114, 594–604. doi:10.1175/1520-0493(1986)114<0594:IVOTAS>2.0.CO;2.

Hourdin, F., Musat, I., Guichard, F. se, Ruti, P. M., Favot, F., Filiberti, M.-A., et al. (2010). AMMA-Model Intercomparison Project. *Bull. Am. Meteorol. Soc.* 91, 95–104. doi:10.1175/2009BAMS2791.1.

Huang, D.-Q., Zhu, J., Zhang, Y.-C., and Huang, A.-N. (2013). Uncertainties on the simulated summer precipitation over Eastern China from the CMIP5 models. *J. Geophys. Res. Atmos.* 118, 9035–9047. doi:10.1002/jgrd.50695.

Huang, R., Zhou, L., and Chen, W. (2003). The Progresses of Recent Studies on the Variabilities of the East Asian Monsoon and Their Causes. *Adv. Atmos. Sci.* 20, 55–69. doi:10.1007/BF03342050.

Hunt, K. M. R., Turner, A. G., and Shaffrey, L. C. (2018). The evolution, seasonality and impacts of western disturbances. *Q. J. R. Meteorol. Soc.* 144, 278–290. doi:10.1002/qj.3200.

Janicot, S., Mounier, F., Gervois, S., Sultan, B., and Kiladis, G. N. (2010). The Dynamics of the West African Monsoon. Part V: The Detection and Role of the Dominant Modes of Convectively Coupled Equatorial Rossby Waves. *J. Clim.* 23, 4005–4024. doi:10.1175/2010JCLI3221.1.

Jiang, D. (2005). Natural interdecadal weakening of East Asian summer monsoon in the late 20th century. *Chinese Sci. Bull.* 50, 1923. doi:10.1360/982005-36.

Jiang, D., Hu, D., Tian, Z., and Lang, X. (2020). Differences between CMIP6 and CMIP5 Models in Simulating Climate over China and the East Asian Monsoon. *Adv. Atmos. Sci.* 37, 1102–1118. doi:10.1007/s00376-020-2034-y.

Jiang, D., Tian, Z., and Lang, X. (2016). Reliability of climate models for China through the IPCC Third to Fifth Assessment Reports. *Int. J. Climatol.* 36, 1114–1133. doi:10.1002/joc.4406.

Jiao, Y., Wu, R., and Song, L. (2019). Individual and Combined Impacts of Two Eurasian Wave Trains on Intraseasonal East Asian Winter Monsoon Variability. *J. Geophys. Res. Atmos.* 124, 4530–4548. doi:10.1029/2018JD029953.

Jin, Q., Yang, X.-Q., Sun, X.-G., and Fang, J.-B. (2013). East Asian summer monsoon circulation structure controlled by feedback of condensational heating. *Clim. Dyn.* 41, 1885–1897. doi:10.1007/s00382-012-1620-9.

Joetzjer, E., Douville, H., Delire, C., and Ciais, P. (2013). Present-day and future Amazonian precipitation in global climate models: CMIP5 versus CMIP3. *Clim. Dyn.* 41, 2921–2936. doi:10.1007/s00382-012-1644-1.

Jones, C., and Carvalho, L. M. V. (2002). Active and Break Phases in the South American Monsoon System. *J. Clim.* 15, 905–914. doi:10.1175/1520-0442(2002)015<0905:AABPIT>2.0.CO;2.

Jones, C., and Carvalho, L. M. V (2013). Climate Change in the South American Monsoon System: Present Climate and CMIP5 Projections. *J. Clim.* 26, 6660–6678. doi:10.1175/JCLI-D-12-00412.1.

Kikuchi, K., Wang, B., and Kajikawa, Y. (2012). Bimodal representation of the tropical intraseasonal oscillation. *Clim. Dyn.* 38, 1989–2000. doi:10.1007/s00382-011-1159-1.

Kim, H.-J., Wang, B., and Ding, Q. (2008). The Global Monsoon Variability Simulated by CMIP3 Coupled Climate Models. *J. Clim.* 21, 5271–5294. doi:10.1175/2008JCLI2041.1.

Kitoh et al., Kitoh, A., Endo, H., Krishna Kumar, K., Cavalcanti, I. F. A., Goswami, P., et al. (2013). Monsoons in a changing world: A regional perspective in a global context. *J. Geophys. Res. Atmos.* 118, 3053–3065. doi:10.1002/jgrd.50258.

Kodama, Y. (1992). Large-Scale Common Features of Subtropical Precipitation Zones (the Baiu Frontal Zone, the SPCZ, and the SACZ) Part I: Characteristics of Subtropical Frontal Zones. *J. Meteorol. Soc. Japan. Ser. II* 70, 813–836. doi:10.2151/jmsj1965.70.4_813.

Kosaka, Y., Xie, S.-P., Lau, N.-C., and Vecchi, G. A. (2013). Origin of seasonal predictability for summer climate over the Northwestern Pacific. *Proc. Natl. Acad. Sci.* 110, 7574–7579. doi:10.1073/pnas.1215582110.

Krishnan, R., Sabin, T. P., Madhura, R. K., Vellore, R. K., Mujumdar, M., Sanjay, J., et al. (2019a). Non-monsoonal precipitation response over the Western Himalayas to climate change. *Clim. Dyn.* 52, 4091–4109. doi:10.1007/s00382-018-4357-2.

Krishnan, R., Shrestha, A. B., Ren, G., Rajbhandari, R., Saeed, S., Sanjay, J., et al. (2019b). “Unravelling Climate Change in the Hindu Kush Himalaya: Rapid Warming in the Mountains and Increasing Extremes,” in *The Hindu Kush Himalaya Assessment*, eds. P. Wester, A. Mishra, A. Mukherji, and A. B. Shrestha (Cham: Springer International Publishing), 57–97. doi:10.1007/978-3-319-92288-1_3.

Lafore, J.-P., Beucher, F., Peyrillé, P., Diongue-Niang, A., Chapelon, N., Bouniol, D., et al. (2017). A multi-scale analysis of the extreme rain event of Ouagadougou in 2009. *Q. J. R. Meteorol. Soc.* 143, 3094–3109. doi:10.1002/qj.3165.

Lamb, P. J. (1978). Large-scale Tropical Atlantic surface circulation patterns associated with Subsaharan weather anomalies. *Tellus* 30, 240–251. doi:10.3402/tellusa.v30i3.10338.

Lee, E.-J., Yeh, S.-W., Jhun, J.-G., and Moon, B.-K. (2006). Seasonal change in anomalous WNPSH associated with the strong East Asian summer monsoon. *Geophys. Res. Lett.* 33, L21702. doi:10.1029/2006GL027474.

Lee, J.-Y., Kwon, M., Yun, K.-S., Min, S.-K., Park, I.-H., Ham, Y.-G., et al. (2017). The long-term variability of Changma in the East Asian summer monsoon system: A review and revisit. *Asia-Pacific J. Atmos. Sci.* 53, 257–272. doi:10.1007/s13143-017-0032-5.

Lee, J.-Y., Wang, B., Wheeler, M. C., Fu, X., Waliser, D. E., and Kang, I.-S. (2013a). Real-time multivariate indices for the boreal summer intraseasonal oscillation over the Asian summer monsoon region. *Clim. Dyn.* 40, 493–509. doi:10.1007/s00382-012-1544-4.

Lee, S.-S., Seo, Y.-W., Ha, K.-J., and Jhun, J.-G. (2013b). Impact of the western North Pacific subtropical high on the East Asian monsoon precipitation and the Indian Ocean precipitation in the boreal summertime. *Asia-Pacific J. Atmos. Sci.* 49, 171–182. doi:10.1007/s13143-013-0018-x.

Lenters, J. D., and Cook, K. H. (1997). On the Origin of the Bolivian High and Related Circulation Features of the South American Climate. *J. Atmos. Sci.* 54, 656–678. doi:10.1175/1520-0469(1997)054<0656:OTOOTB>2.0.CO;2.

Levine, R. C., Turner, A. G., Marathayil, D., and Martin, G. M. (2013). The role of northern Arabian Sea surface temperature biases in CMIP5 model simulations and future projections of Indian summer monsoon rainfall. *Clim. Dyn.* 41, 155–172. doi:10.1007/s00382-012-1656-x.

Li, W., and Fu, R. (2004). Transition of the Large-Scale Atmospheric and Land Surface Conditions from the Dry to the Wet Season over Amazonia as Diagnosed by the ECMWF Re-Analysis. *J. Clim.* 17, 2637–2651. doi:10.1175/1520-0442(2004)017<2637:TOTLAA>2.0.CO;2.

Li, X., Gollan, G., Greatbatch, R. J., and Lu, R. (2018). Intraseasonal variation of the East Asian summer monsoon associated with the Madden-Julian Oscillation. *Atmos. Sci. Lett.* 19, e794. doi:10.1002/asl.794.

Liebmann, B., Kiladis, G. N., Vera, C. S., Saulo, A. C., and Carvalho, L. M. V. (2004). Subseasonal Variations of Rainfall in South America in the Vicinity of the Low-Level Jet East of the Andes and Comparison to Those in the South Atlantic Convergence Zone. *J. Clim.* 17, 3829–3842. doi:10.1175/1520-0442(2004)017<3829:SVORIS>2.0.CO;2.

Luo, X., and Wang, B. (2019). How autumn Eurasian snow anomalies affect east asian winter monsoon: a numerical study. *Clim. Dyn.* 52, 69–82. doi:10.1007/s00382-018-4138-y.

Madhura, R. K., Krishnan, R., Revadekar, J. V., Mujumdar, M., and Goswami, B. N. (2014). Changes in western disturbances over the Western Himalayas in a warming environment. *Clim. Dyn.* 44, 1157–1168. doi:10.1007/s00382-014-2166-9.

Man, W., Zhou, T., and Jungclaus, J. H. (2012). Simulation of the East Asian Summer Monsoon during the Last Millennium with the MPI Earth System Model. *J. Clim.* 25, 7852–7866. doi:10.1175/JCLI-D-11-00462.1.

Marengo, J. ., Nobre, C. ., Tomasella, J., Cardoso, M. ., and Oyama, M. . (2008). Hydro-climatic and ecological behaviour of the drought of Amazonia in 2005. *Philos. Trans. R. Soc. B Biol. Sci.* 363, 1773–1778. doi:10.1098/rstb.2007.0015.

Marengo, J. A., Liebmann, B., Grimm, A. M., Misra, V., Silva Dias, P. L., Cavalcanti, I. F. A., et al. (2012). Recent developments on the South American monsoon system. *Int. J. Climatol.* 32, 1–21. doi:10.1002/joc.2254.

McBride, J. L. (1987). “The Australian summer monsoon,” in *Monsoon Meteorology*, eds. C. Chang and T. Kristinamurti (Oxford University Press), 203–231.

McBride, J. L., and Nicholls, N. (1983). Seasonal Relationships between Australian Rainfall and the Southern Oscillation. *Mon. Weather Rev.* 111, 1998–2004. doi:10.1175/1520-0493(1983)111<1998:SRBARA>2.0.CO;2.

Mekonnen, A., Thorncroft, C. D., Aiyyer, A. R., and Kiladis, G. N. (2008). Convectively Coupled Kelvin Waves over Tropical Africa during the Boreal Summer: Structure and Variability. *J. Clim.* 21, 6649–6667. doi:10.1175/2008JCLI2008.1.

Miao, J., Wang, T., Wang, H., Zhu, Y., and Sun, J. (2018). Interdecadal Weakening of the East Asian Winter Monsoon in the Mid-1980s: The Roles of External Forcings. *J. Clim.* 31, 8985–9000. doi:10.1175/JCLI-D-17-0868.1.

Miao, J., Wang, T., Zhu, Y., Min, J., Wang, H., and Guo, D. (2016). Response of the East Asian Winter Monsoon to Strong Tropical Volcanic Eruptions. *J. Clim.* 29, 5041–5057. doi:10.1175/JCLI-D-15-0600.1.

Moise, A. F., Colman, R. A., and Brown, J. R. (2012). Behind uncertainties in projections of Australian tropical climate: Analysis of 19 CMIP3 models. *J. Geophys. Res. Atmos.* 117, n/a-n/a. doi:10.1029/2011JD017365.

Monerie, P.-A., Wainwright, C. M., Sidibe, M., and Akinsanola, A. A. (2020). Model uncertainties in climate change impacts on Sahel precipitation in ensembles of CMIP5 and CMIP6 simulations. *Clim. Dyn.* doi:10.1007/s00382-020-05332-0.

Narsey, S. Y., Brown, J. R., Colman, R. A., Delage, F., Power, S. B., Moise, A. F., et al. (2020). Climate Change Projections for the Australian Monsoon From CMIP6 Models. *Geophys. Res. Lett.* 47, e2019GL086816. doi:https://doi.org/10.1029/2019GL086816.

Nicholls, N., McBride, J. L., and Ormerod, R. J. (1982). On Predicting the Onset of the Australian Wet Season at Darwin. *Mon. Weather Rev.* 110, 14–17. doi:10.1175/1520-0493(1982)110<0014:OPTOOT>2.0.CO;2.

Nicholson, S. E. (2017). Climate and climatic variability of rainfall over eastern Africa. *Rev. Geophys.* 55, 590–635. doi:10.1002/2016RG000544.

Nicholson, S. E., Fink, A. H., and Funk, C. (2018). Assessing recovery and change in West Africa’s rainfall regime from a 161-year record. *Int. J. Climatol.* 38, 3770–3786. doi:10.1002/joc.5530.

Nitta, T. (1987). Convective Activities in the Tropical Western Pacific and Their Impact on the Northern Hemisphere Summer Circulation. *J. Meteorol. Soc. Japan. Ser. II* 65, 373–390. doi:10.2151/jmsj1965.65.3_373.

Novello, V. F., Cruz, F. W., Vuille, M., Stríkis, N. M., Edwards, R. L., Cheng, H., et al. (2017). A high-resolution history of the South American Monsoon from Last Glacial Maximum to the Holocene. *Sci. Rep.* 7, 1–8. doi:10.1038/srep44267.

Omotosho, J. ’Bay. (1988). Spatial variation of rainfall in Nigeria during the ‘little dry season.’ *Atmos. Res.* 22, 137–147. doi:10.1016/0169-8095(88)90004-X.

Paegle, J. N., and Mo, K. C. (2002). Linkages between Summer Rainfall Variability over South America and Sea Surface Temperature Anomalies. *J. Clim.* 15, 1389–1407. doi:10.1175/1520-0442(2002)015<1389:LBSRVO>2.0.CO;2.

Pai, D. S., Bangdar, A., Devi, S., Musale, M., Badwik, M., Kundale, A. P., et al. (2020). Normal dates of onset/progress and wthdrawal of southwest monsoon over India. *Mausam* 71, 553–570.

Pant, G., and Rupa Kumar, K. (1997). *Climates of South Asia*. John Wiley and Sons Ltd.

Pascale, S., Boos, W. R., Bordoni, S., Delworth, T. L., Kapnick, S. B., Murakami, H., et al. (2017). Weakening of the North American monsoon with global warming. *Nat. Clim. Chang.* 7, 806–812. doi:10.1038/nclimate3412.

Pascale, S., Carvalho, L. M. V. V, Adams, D. K., Castro, C. L., and Cavalcanti, I. F. A. A. (2019). Current and Future Variations of the Monsoons of the Americas in a Warming Climate. *Curr. Clim. Chang. Reports* 5, 125–144. doi:10.1007/s40641-019-00135-w.

Peng, Y., Shen, C., Wang, W.-C., and Xu, Y. (2010). Response of Summer Precipitation over Eastern China to Large Volcanic Eruptions. *J. Clim.* 23, 818–824. doi:10.1175/2009JCLI2950.1.

Raia, A., and Cavalcanti, I. F. A. (2008). The Life Cycle of the South American Monsoon System. *J. Clim.* 21, 6227–6246. doi:10.1175/2008JCLI2249.1.

Raj, J., Bangalath, H. K., and Stenchikov, G. (2019). West African Monsoon: current state and future projections in a high-resolution AGCM. *Clim. Dyn.* 52, 6441–6461. doi:10.1007/s00382-018-4522-7.

Reed, T. R. (1933). The North American high-level anticyclone. *Mon. Wea. Rev.* 61, 321–325. doi:10.1175/1520-0493(1933)61<321:TNAHA>2.0.CO;2.

Risanto, C. B., Castro, C. L., Moker, J. M., Arellano, A. F., Adams, D. K., Fierro, L. M., et al. (2019). Evaluating forecast skills of moisture from convective-permitting WRF-ARW Model during 2017 North American Monsoon season. *Atmosphere (Basel).* doi:10.3390/atmos10110694.

Robertson, A. W., and Mechoso, C. R. (2000). Interannual and Interdecadal Variability of the South Atlantic Convergence Zone. *Mon. Weather Rev.* 128, 2947–2957. doi:10.1175/1520-0493(2000)128<2947:IAIVOT>2.0.CO;2.

Robertson, A. W., Moron, V., Qian, J.-H., Chang, C.-P., Tangang, F., Aldrian, E., et al. (2011). "The Maritime Continent Monsoon," in, 85–98. doi:10.1142/9789814343411_0006.

Roehrig, R., Bouniol, D., Guichard, F., Hourdin, F., and Redelsperger, J.-L. L. (2013). The present and future of the west african monsoon: A process-oriented assessment of cmip5 simulations along the amma transect. *J. Clim.* 26, 6471–6505. doi:10.1175/JCLI-D-12-00505.1.

Roehrig, R., Chauvin, F., and Lafore, J.-P. (2011). 10–25-Day Intraseasonal Variability of Convection over the Sahel: A Role of the Saharan Heat Low and Midlatitudes. *J. Clim.* 24, 5863–5878. doi:10.1175/2011JCLI3960.1.

Rojas, M., Arias, P. A., Flores-Aqueveque, V., Seth, A., and Vuille, M. (2016). The South American monsoon variability over the last millennium in climate models. *Clim. Past* 12, 1681–1691. doi:10.5194/cp-12-1681-2016.

Sabeerali, C. T., Ramu Dandi, A., Dhakate, A., Salunke, K., Mahapatra, S., and Rao, S. A. (2013). Simulation of boreal summer intraseasonal oscillations in the latest CMIP5 coupled GCMs. *J. Geophys. Res. Atmos.* 118, 4401–4420. doi:10.1002/jgrd.50403.

Sandeep, S., and Ajayamohan, R. S. (2015). Origin of cold bias over the Arabian Sea in Climate Models. *Sci. Rep.* 4, 6403. doi:10.1038/srep06403.

Shige, S., Nakano, Y., and Yamamoto, M. K. (2017). Role of Orography, Diurnal Cycle, and Intraseasonal Oscillation in Summer Monsoon Rainfall over the Western Ghats and Myanmar Coast. *J. Clim.* 30, 9365–9381. doi:10.1175/JCLI-D-16-0858.1.

Silvestri, G. E. (2003). Antarctic Oscillation signal on precipitation anomalies over southeastern South America. *Geophys. Res. Lett.* 30, 2115. doi:10.1029/2003GL018277.

Silvestri, G., and Vera, C. (2009). Nonstationary Impacts of the Southern Annular Mode on Southern Hemisphere Climate. *J. Clim.* 22, 6142–6148. doi:10.1175/2009JCLI3036.1.

Song, F., and Zhou, T. (2013). FGOALS-s2 simulation of upper-level jet streams over East Asia: Mean state bias and synoptic-scale transient eddy activity. *Adv. Atmos. Sci.* 30, 739–753. doi:10.1007/s00376-012-2212-7.

Song, F., and Zhou, T. (2014). The Climatology and Interannual Variability of East Asian Summer Monsoon in CMIP5 Coupled Models: Does Air–Sea Coupling Improve the Simulations? *J. Clim.* 27, 8761–8777. doi:10.1175/JCLI-D-14-00396.1.

Song, F., Zhou, T., and Wang, L. (2013). Two modes of the silk road pattern and their interannual variability simulated by LASG/IAP AGCM SAMIL2.0. *Adv. Atmos. Sci.* 30, 908–921. doi:10.1007/s00376-012-2145-1.

Sow, M., Diakhaté, M., Dixon, R. D., Guichard, F., Dieng, D., and Gaye, A. T. (2020). Uncertainties in the Annual Cycle of Rainfall Characteristics over West Africa in CMIP5 Models. *Atmosphere (Basel).* 11, 216. doi:10.3390/atmos11020216.

Sperber, K. R., Annamalai, H., Kang, I.-S., Kitoh, A., Moise, A., Turner, A., et al. (2013). The Asian summer monsoon: an intercomparison of CMIP5 vs. CMIP3 simulations of the late 20th century. *Clim. Dyn.* 41, 2711–2744. doi:10.1007/s00382-012-1607-6.

Stensrud, D. J., Gall, R. L., and Nordquist, M. K. (1997). Surges over the Gulf of California during the Mexican Monsoon. *Mon. Weather Rev.* 125, 417–437. doi:10.1175/1520-0493(1997)125<0417:SOTGOC>2.0.CO;2.

Sultan, B., and Janicot, S. (2003). The West African Monsoon Dynamics. Part II: The "Preonset" and "Onset" of the Summer Monsoon. *J. Clim.* 16, 3407–3427. doi:10.1175/1520-0442(2003)016<3407:TWAMDP>2.0.CO;2.

Suppiah, R. (1992). The Australian summer monsoon: a review. *Prog. Phys. Geogr. Earth Environ.* 16, 283–318. doi:10.1177/030913339201600302.

Sylla, M. B., Gaye, A. T., Jenkins, G. S., Pal, J. S., and Giorgi, F. (2010). Consistency of projected drought over the Sahel with changes in the monsoon circulation and extremes in a regional climate model projections. *J. Geophys. Res.* 115, D16108. doi:10.1029/2009JD012983.

Torres-Alavez, A., Cavazos, T., and Turrent, C. (2014). Land-sea thermal contrast and intensity of the North American monsoon under climate change conditions. *J. Clim.* 27, 4566–4580. doi:10.1175/JCLI-D-13-00557.1.

Troup, A. (1961). Variations in upper troposheric flow associated with the onset of the Australian summer monsoon. *Indian J. Meteorol. Geophys.* 12, 217–230.

Turner, A. G., and Annamalai, H. (2012). Climate change and the South Asian summer monsoon. *Nat. Clim. Chang.* 2, 587–595. doi:10.1038/nclimate1495.

Varuolo-Clarke, A. M., Reed, K. A., and Medeiros, B. (2019). Characterizing the North American Monsoon in the Community Atmosphere Model: Sensitivity to Resolution and Topography. *J. Clim.* 32, 8355–8372. doi:10.1175/JCLI-D-18-0567.1.

Vera, C., Higgins, W., Amador, J., Ambrizzi, T., Garreaud, R., Gochis, D., et al. (2006). Toward a Unified View of the American Monsoon Systems. *J. Clim.* 19, 4977–5000. doi:10.1175/JCLI3896.1.

Vizy, E. K., and Cook, K. H. (2009). A mechanism for African monsoon breaks: Mediterranean cold air surges. *J. Geophys. Res. Atmos.* 114. doi:10.1029/2008JD010654.

Vuille, M., Burns, S. J., Taylor, B. L., Cruz, F. W., Bird, B. W., Abbott, M. B., et al. (2012). A review of the South American monsoon history as recorded in stable isotopic proxies over the past two millennia. *Clim. Past* 8, 1309–1321. doi:10.5194/cp-8-1309-2012.

Wang, B. (2005). Fundamental challenge in simulation and prediction of summer monsoon rainfall. *Geophys. Res. Lett.* 32, L15711. doi:10.1029/2005GL022734.

Wang, B., and Ding, Q. (2008). Global monsoon: Dominant mode of annual variation in the tropics. *Dyn. Atmos. Ocean.* 44, 165–183. doi:10.1016/j.dynatmoce.2007.05.002.

Wang, B., and LinHo (2002). Rainy Season of the Asian–Pacific Summer Monsoon*. *J. Clim.* 15, 386–398. doi:10.1175/1520-0442(2002)015<0386:RSOTAP>2.0.CO;2.

Wang, B., Wu, R., and Fu, X. (2000). Pacific–East Asian Teleconnection: How Does ENSO Affect East Asian Climate? *J. Clim.* 13, 1517–1536. doi:10.1175/1520-0442(2000)013<1517:PEATHD>2.0.CO;2.

Wang, B., Wu, Z., Chang, C.-P., Liu, J., Li, J., and Zhou, T. (2010). Another Look at Interannual-to-Interdecadal Variations of the East Asian Winter Monsoon: The Northern and Southern Temperature Modes. *J. Clim.* 23, 1495–1512. doi:10.1175/2009JCLI3243.1.

Wang, B., Xiang, B., and Lee, J.-Y. (2013). Subtropical High predictability establishes a promising way for monsoon and tropical storm predictions. *Proc. Natl. Acad. Sci.* 110, 2718–2722. doi:10.1073/pnas.1214626110.

Wang, H., and Fu, R. (2002). Cross-Equatorial Flow and Seasonal Cycle of Precipitation over South America. *J. Clim.* 15, 1591–1608. doi:10.1175/1520-0442(2002)015<1591:CEFASC>2.0.CO;2.

Wang, H., and He, S. (2012). Weakening relationship between East Asian winter monsoon and ENSO after mid-1970s. *Chinese Sci. Bull.* 57, 3535–3540. doi:10.1007/s11434-012-5285-x.

Wang, L., and Chen, W. (2014). The East Asian winter monsoon: re-amplification in the mid-2000s. *Chinese Sci. Bull.* 59, 430–436. doi:10.1007/s11434-013-0029-0.

Wang, L., Huang, R., Gu, L., Chen, W., and Kang, L. (2009). Interdecadal Variations of the East Asian Winter Monsoon and Their Association with Quasi-Stationary Planetary Wave Activity. *J. Clim.* 22, 4860–4872. doi:10.1175/2009JCLI2973.1.

Wang, P. X., Wang, B., Cheng, H., Fasullo, J., Guo, Z. T., Kiefer, T., et al. (2014). The global monsoon across timescales: coherent variability of regional monsoons. *Clim. Past* 10, 2007–2052. doi:10.5194/cp-10-2007-2014.

Wang, P. X., Wang, B., Cheng, H., Fasullo, J., Guo, Z. T., Kiefer, T., et al. (2017). The global monsoon across time scales: Mechanisms and outstanding issues. *Earth-Science Rev.* doi:10.1016/j.earscirev.2017.07.006.

Wang, T., Miao, J.-P., Sun, J.-Q., and Fu, Y.-H. (2018). Intensified East Asian summer monsoon and associated precipitation mode shift under the 1.5 °C global warming target. *Adv. Clim. Chang. Res.* 9, 102–111. doi:10.1016/j.accre.2017.12.002.

Webster, P. J., Magaña, V. O., Palmer, T. N., Shukla, J., Tomas, R. A., Yanai, M., et al. (1998). Monsoons: Processes, predictability, and the prospects for prediction. *J. Geophys. Res. Ocean.* 103, 14451–14510. doi:10.1029/97JC02719.

Wen, C., Graf, H.-F., and Ronghui, H. (2000). The interannual variability of East Asian Winter Monsoon and its relation to the summer monsoon. *Adv. Atmos. Sci.* 17, 48–60. doi:10.1007/s00376-000-0042-5.

Wen, X., Liu, Z., Wang, S., Cheng, J., and Zhu, J. (2016). Correlation and anti-correlation of the East Asian summer and winter monsoons during the last 21,000 years. *Nat. Commun.* 7, 11999. doi:10.1038/ncomms11999.

Xue, Y., De Sales, F., Lau, W. K.-M., Boone, A., Feng, J., Dirmeyer, P., et al. (2010). Intercomparison and analyses of the climatology of the West African Monsoon in the West African Monsoon Modeling and Evaluation project (WAMME) first model intercomparison experiment. *Clim. Dyn.* 35, 3–27. doi:10.1007/s00382-010-0778-2.

Yan, M., Liu, Z. Y., Ning, L., and Liu, J. (2020). Holocene EASM-EAWM Relationship Across Different Timescales in CCSM3. *Geophys. Res. Lett.* 47. doi:10.1029/2020GL088451.

Yasunari, T. (1979). Cloudiness Fluctuations Associated with the Northern Hemisphere Summer Monsoon. *J. Meteorol. Soc. Japan. Ser. II* 57, 227–242. doi:10.2151/jmsj1965.57.3_227.

Yihui, D., and Chan, J. C. L. (2005). The East Asian summer monsoon: an overview. *Meteorol. Atmos. Phys.* 89, 117–142. doi:10.1007/s00703-005-0125-z.

Yim, S.-Y., Yeh, S.-W., Wu, R., and Jhun, J.-G. (2008). The Influence of ENSO on Decadal Variations in the Relationship between the East Asian and Western North Pacific Summer Monsoons. *J. Clim.* 21, 3165–3179. doi:10.1175/2007JCLI1948.1.

Yin, L., Fu, R., Zhang, Y.-F., Arias, P. A., Fernando, D. N., Li, W., et al. (2014). What controls the interannual variation of the wet season onsets over the Amazon? *J. Geophys. Res. Atmos.* 119, 2314–2328. doi:10.1002/2013JD021349.

Zeng, N., Yoon, J.-H., Marengo, J. A., Subramaniam, A., Nobre, C. A., Mariotti, A., et al. (2008). Causes and impacts of the 2005 Amazon drought. *Environ. Res. Lett.* 3, 014002. doi:10.1088/1748-9326/3/1/014002.

Zhang, H., and Moise, A. (2016). "The Australian summer monsoon in current and future climate," in *The Monsoons and Climate Change*, eds. C. Jones and L. Carvalho (Berlin: Springer, , doi.org/10.1007/978-3-319-21650-8_5), 67–120.

Zhang, L., Wang, B., and Zeng, Q. (2009). Impact of the Madden–Julian Oscillation on Summer Rainfall in Southeast China. *J. Clim.* 22, 201–216. doi:10.1175/2008JCLI1959.1.

Zhang, Z., Chan, J. C. L., and Ding, Y. (2004). Characteristics, evolution and mechanisms of the summer monsoon onset over Southeast Asia. *Int. J. Climatol.* 24, 1461–1482. doi:10.1002/joc.1082.

Zhou, J., and Lau, K.-M. (1998). Does a Monsoon Climate Exist over South America? *J. Clim.* 11, 1020–1040. doi:10.1175/1520-0442(1998)011<1020:DAMCEO>2.0.CO;2.

Zhou, T., Gong, D., Li, J., and Li, B. (2009). Detecting and understanding the multi-decadal variability of the East Asian Summer Monsoon Recent progress and state of affairs. *Meteorol. Zeitschrift* 18, 455–467. doi:10.1127/0941-2948/2009/0396.

Zhou, T., Turner, A. G., Kinter, J. L., Wang, B., Qian, Y., Chen, X., et al. (2016). GMMIP (v1.0) contribution to CMIP6: Global Monsoons Model Inter-comparison Project. *Geosci. Model Dev.* 9, 3589–3604. doi:10.5194/gmd-9-3589-2016.

Figures

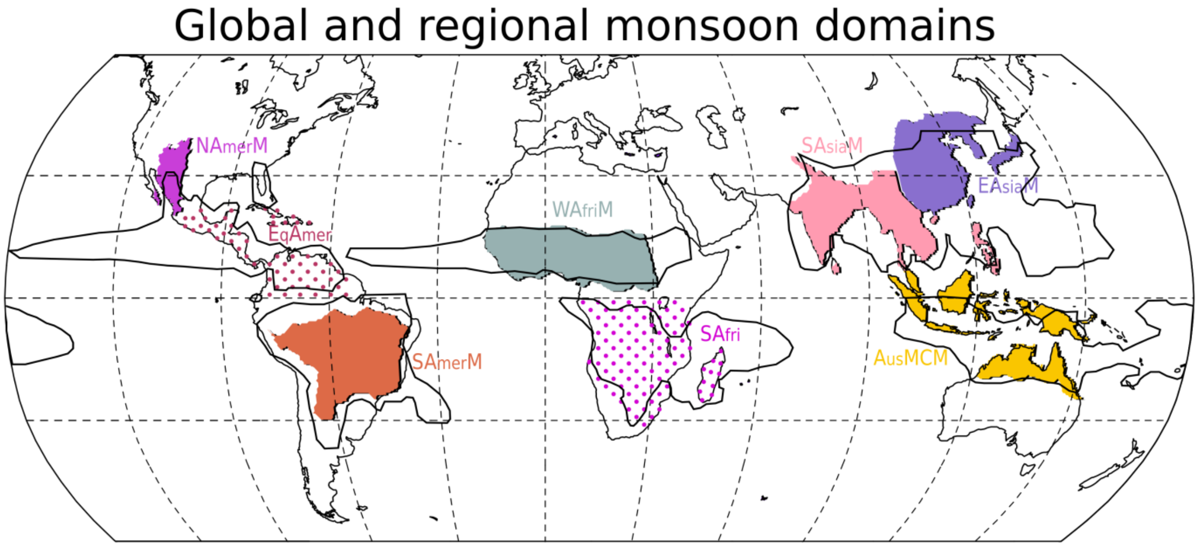

Figure AV.1: Global and regional monsoons domains. AR6 global monsoon area is represented by the black contour. AR6 regional monsoons are: North American monsoon (shaded magenta), South American monsoon (shaded dark-orange), West African monsoon (shaded grey), South and Southeast Asian monsoon (shaded pink), East Asian monsoon (shaded purple) and Australian-Maritime Continent monsoon (shaded yellow). Areas over Equatorial America and South Africa (dotted red and magenta, respectively) are highlighted but not identified as specific regional monsoons (see explanation in the main text). For each regional monsoon, the seasonal characteristics associated with each domain are specified in the main text.